Scientific Reports

https://doi.org/10.1038/s41598-026-45010-5

Article in Press

Barrier Lyapunov function-based robust adaptive neural network control with dynamically adjusted activation functions for Euler–Lagrange systems under position constraints

Received: 2 July 2025

Accepted: 16 March 2026

Published online: 21 April 2026

Cite this article as: Yilmaz B.M. Barrier Lyapunov function-based robust adaptive neural network control with dynamically adjusted activation functions for Euler–Lagrange systems under position constraints. *Sci Rep* (2026). https://doi.org/10.1038/s41598-026-45010-5

Bayram Melih Yilmaz

We are providing an unedited version of this manuscript to give early access to its findings. Before final publication, the manuscript will undergo further editing. Please note there may be errors present which affect the content, and all legal disclaimers apply.

If this paper is publishing under a Transparent Peer Review model then Peer Review reports will publish with the final article.

ARTICLE IN PRESS

© The Author(s) 2026. **Open Access** This article is licensed under a Creative Commons Attribution-NonCommercial-NoDerivatives 4.0 International License, which permits any non-commercial use, sharing, distribution and reproduction in any medium or format, as long as you give appropriate credit to the original author(s) and the source, provide a link to the Creative Commons licence, and indicate if you modified the licensed material. You do not have permission under this licence to share adapted material derived from this article or parts of it. The images or other third party material in this article are included in the article's Creative Commons licence, unless indicated otherwise in a credit line to the material. If material is not included in the article's Creative Commons licence and your intended use is not permitted by statutory regulation or exceeds the permitted use, you will need to obtain permission directly from the copyright holder. To view a copy of this licence, visit http://creativecommons.org/licenses/by-nc-nd/4.0/.

ARTICLE IN PRESS

Barrier Lyapunov Function-Based Robust Adaptive Neural Network Control with Dynamically Adjusted Activation Functions for Euler-Lagrange Systems under Position Constraints

Bayram Melih Yilmaz[1,*]

[1]Bayram Melih Yilmaz, Department of Electrical Engineering, Manisa Celal Bayar University, 45400, Turgutlu, Manisa, Türkiye.
[*]melih.yilmaz@cbu.edu.tr

ABSTRACT

This paper proposes a novel robust control strategy with position constraints for a class of Euler–Lagrange systems. The approach integrates an adaptive neural network estimator to compensate for parametric uncertainties while ensuring accurate trajectory tracking. A key feature of the proposed method is the iterative online adjustment of the activation function centers in the neural networks, which significantly enhances its ability to capture time-varying nonlinearities—beyond what conventional fixed-center neural network structures can achieve. The primary objective is to guarantee precise trajectory tracking, while the secondary objective is to ensure that the tracking error remains strictly within a predefined region, thereby regulating transient behavior and limiting overshoot. To achieve this, a barrier Lyapunov function is incorporated into the control design, enforcing state constraints and ensuring that all closed-loop signals remain bounded. Rigorous Lyapunov-based stability analysis is provided, and numerical simulations on a two degree of freedom robotic manipulator demonstrate the effectiveness and robustness of the proposed control framework under system uncertainties and external disturbances.

ARTICLE IN PRESS

1 Introduction

The increasing integration of mechatronic systems in industry has led to a growing body of research on the control of these systems in the scientific literature[1,2]. At the core of these systems are Euler-Lagrange systems, which are utilized to perform specific tasks under challenging conditions. Euler-Lagrange systems are well-defined multi-input/multi-output nonlinear models[3], yet their parameters are often uncertain in practice. One of the most commonly used techniques for managing systems with parametric uncertainties is robust control algorithm. Some robust control designs that compensate for uncertainties by suppression are presented in[4–6]. Another control algorithm is adaptive control for linearly parameterizable systems[7,8]. This control strategy enhances efficiency by estimating and compensating for model uncertainties rather than merely suppressing them. However, it requires a regressor matrix, which can be computationally intensive to generate for certain Euler-Lagrange systems and is highly system-dependent.

Another method for compensating model and disturbance uncertainties is the neural network (NN), which leverages its universal approximation properties[9–12]. Alternatively, the fuzzy logic algorithm is also employed to address both model and disturbance uncertainties[13,14]. To address uncertainties, the framework can employ either an offline lookup table strategy or real-time estimation. Specifically, a fuzzy-based method that dynamically adjusts the means and variances of membership functions for each input can significantly improve performance.

In standard artificial NN, activation functions usually have fixed centers, which restricts their ability to adapt to dynamic changes in system behavior. In contrast, activation functions with dynamically adjustable centers can improve the network's adaptability and learning performance by modulating their responsiveness according to the magnitude of the tracking error. In a recent study[15], a heterogeneous memristive Hopfield NN was introduced, incorporating both fixed and memristor-driven adaptive activation functions. Although these activation functions exhibit dynamic behavior as a result of the memristor's internal state changes, no explicit online update law is employed—the adaptivity arises passively from memristive dynamics. In[16], the authors propose adaptive activation functions incorporating a tunable hyperparameter to improve the expressiveness of deep and physics-informed NN, particularly for approximating both smooth and discontinuous solutions of partial differential equations. However, the work did not provide stability analysis. In[17], Kronecker NNs are introduced as a flexible framework that allows the integration of adaptive activation functions across different NN architectures. Despite the enhanced adaptability, the study did not provide a formal stability analysis.

ARTICLE IN PRESS

The stability conditions of closed-loop nonlinear systems are investigated using a Lyapunov-based algorithm. Certain approaches are limited to guaranteeing the system's steady-state behavior. Nevertheless, managing the overshoot in tracking errors is crucial, particularly in industrial applications. To address this challenge, the barrier Lyapunov function (BLF) based stability technique is employed for ensuring the stability of closed-loop systems.[18] has presented a BLF-based control design for nonlinear systems with output constraints. Similarly,[19] proposed an adaptive backstepping controller employing the BLF approach. Additionally,[20] proposed a sliding-mode control design that ensures finite-time stability and state constraint satisfaction for nonlinear systems with Lagrangian structures.[21] demonstrates BLF-based fuzzy backstepping control approach for nonlinear systems with full-state constraints. In addition,[22] proposed a robust control strategy for kinematically redundant manipulators using a BLF framework, ensuring task-space errors remain within predefined safe regions with guaranteed transient performance under uncertainties.[23] proposes a neuro-adaptive backstepping control scheme that simultaneously handles input saturation, system uncertainties, and limited state feedback. In addition,[24] presented an adaptive model-free approach for actuated ankle–foot orthoses using a projection-based PID controller with finite-time stability, while[25] developed a decentralized event-triggered fault-tolerant controller with echo-state networks to address actuator faults, disturbances, and input saturation.

The proposed control framework is designed with two main objectives. First, it ensures accurate trajectory tracking of Euler–Lagrange systems under parametric and dynamic uncertainties. Second, it guarantees that the tracking error remains strictly within a predefined bound, thereby regulating transient performance and eliminating overshoot. These objectives are achieved by integrating a BLF, which enforces state constraints, with an adaptive NN that employs self-adjusting activation functions based on a piecewise third-order polynomial. The online adjustment of activation centers enables the NN to effectively approximate time-varying nonlinearities, while the BLF ensures safety by constraining the error dynamics. Together, these elements form a robust control structure that maintains stability and boundedness of all closed-loop signals.

This paper proposes a novel robust control strategy with position constraints for a class of Euler–Lagrange systems subject to dynamic and parametric uncertainties. The primary control objective is to achieve accurate trajectory tracking, while the secondary objective is to ensure that each tracking error—and consequently each joint position—remains within a predefined bound, thereby regulating transient performance and limiting overshoot. To handle uncertainties, an adaptive NN is integrated into the control scheme. Unlike conventional Gaussian-based functions with fixed centers, the proposed NN employs activation functions whose centers are iteratively updated online, improving approximation accuracy near switching or propagation points. A BLF-based approach is employed to enforce position constraints, with a gain matrix dependent on both the tracking and error signals. Stability of the closed-loop system is rigorously established using Lyapunov-based methods, which guarantee uniform ultimate boundedness (UUB) of all system signals. Numerical simulations validate the theoretical findings, demonstrating robust tracking performance under significant uncertainties and disturbances.

The main contributions of this study are summarized below:

- A novel robust control strategy for Euler–Lagrange systems subject to position constraints, which integrates an adaptive neural network with self-adjusting activation functions. This design ensures that the tracking error remains within predefined bounds; unlike prescribed performance control, the constraints are enforced directly via a BLF without error/coordinate transformations.
- A detailed adaptive update mechanism is developed for the NN, where the centers of activation functions are iteratively adjusted online. This enables improved approximation of time-varying uncertainties compared to conventional fixed-activation (e.g., tanh) NNs.
- Introduction of a specially designed piecewise third-order polynomial-based activation function that provides smooth saturation behavior with an adaptively shifting center, improving approximation near switching/propagation regions and reducing control effort.
- A Lyapunov-based stability analysis that establishes invariance of the error inside the admissible set (by the BLF barrier property) and demonstrates boundedness of all closed-loop signals, supported by numerical simulations under uncertainty and disturbances.
- Comprehensive simulations with position-error bounds and comparisons against a well-tuned optimal controller and a fixed-activation NN, evidencing lower tracking error and reduced control effort.

2 System Model and Properties

The mathematical representation of fully actuated n degree of freedom Euler Lagrange system model has following structure[26]

$$M(p)\ddot{p} + C_m(p,\dot{p})\dot{p} + G(p) + F_d\dot{p} + \tau_d = \tau \tag{1}$$

ARTICLE IN PRESS

$p(t)$, $\dot{p}(t)$, $\ddot{p}(t) \in \mathbb{R}^n$ represent position, velocity and acceleration vector, respectively. $M(p) \in \mathbb{R}^{n\times n}$ denotes the inertia matrix, $C_m(p,\dot{p}) \in \mathbb{R}^{n\times n}$ is the centripetal-Coriolis matrix, $G(p) \in \mathbb{R}^n$ includes the gravitational effects, $F_d \in \mathbb{R}^n$ is the viscous frictional effects, $\tau_d(t) \in \mathbb{R}^n$ denotes unknown, bounded disturbance term and $\tau \in \mathbb{R}^n$ is the control torque input.

The use of the Lagrange formulation to derive the dynamics ensures that the inertia matrix $M(p)$ is both positive definite and symmetric, and it adheres to the following inequalities

Property 1 *The inertia matrix $M(p)$ is positive definite, symmetric and satisfies*

$$m_1\|\mu\|^2 \leq \mu^T M(p)\mu \leq m_2\|\mu\|^2 \quad \forall \mu \in \mathbb{R}^n \tag{2}$$

with m_1, $m_2 \in \mathbb{R}$ being positive bounding constants.

Property 2 *The centripetal Coriolis matrix and inertia matrix satisfy the following skew symmetry property*

$$\mu(\dot{M} - 2C_m)\mu = 0 \ \ \forall \mu \in \mathbb{R}^n. \tag{3}$$

3 Development of error system and control design

The primary objective of the control design for the dynamic model given in (1) is to ensure that the actual position signal tracks the desired position signal. In addition to the primary objective of tracking control, there is a secondary objective to ensure that the components of the position tracking error, denoted as $e(t) \in \mathbb{R}^n$, remains within predefined bounds. Specifically, each ith signal must satisfy the condition $\mathscr{D}_i > 0$, implying that

$$|e_i(t)| < \mathscr{D}_i, \ \ i = 1\cdots n, \ \ \forall t > 0. \tag{4}$$

It is equally important to ensure the stability of the closed-loop system by keeping the system signals bounded. In the following analysis, it is assumed that position and velocity signals are measurable. The tracking error in position $e(t)$ is defined as

$$e \triangleq p_d - p \tag{5}$$

where $p_d \in \mathbb{R}^n$ denotes desired position vector. To avoid involving the second derivative of the tracking error explicitly in the control design and stability analysis, a filtered tracking error signal $r(t) \in \mathbb{R}^n$ is introduced, which is defined as

$$r \triangleq \dot{e} + \alpha e \tag{6}$$

where $\alpha \in \mathbb{R}^{n\times n}$ denote positive definite, diagonal, constant gain matrix. After taking the time derivative of (6) and then by multiplying the resultant with M from left, following expression is reached

$$M\dot{r} = -C_m r - \tau + \chi + \tau_d \tag{7}$$

where (1), (6) along with time derivative of (5) were utilized, with $\chi(p,\dot{p},e,\dot{e},\ddot{p}_d) \in \mathbb{R}^n$ being defined as

$$\chi \triangleq M(p)(\ddot{p} + \alpha\dot{e}) + C_m(p,\dot{p})(\dot{p}_d + \alpha e) + G(p) + F_d\dot{q}. \tag{8}$$

Employing the universal approximation property[27,28], It is considered that χ can be modeled using NN as

$$\chi = \omega^T\sigma + \varepsilon \tag{9}$$

where $\omega \in \mathbb{R}^{5n\times n}$ denotes the regression matrix, $\sigma(c,x) \in \mathbb{R}^{5n}$ is the activation function, with $c \in \mathbb{R}^{5n}$ representing the center vector. The input vector is defined as $x \triangleq [p,\dot{p},e,\dot{e},\ddot{p}_d] \in \mathbb{R}^{5n}$. The term $\varepsilon \in \mathbb{R}^n$ stands for the functional approximation error. By employing (9), (7) can be rewritten as

$$M\dot{r} = \omega^T\sigma + \tau_d + \varepsilon - \tau - C_m r. \tag{10}$$

Considering the open-loop dynamics in (7) and the subsequent analysis, the control input is designed as

$$\tau = \hat{\omega}^T\hat{\sigma} + K_e e + K_r r \tag{11}$$

where $K_e \in \mathbb{R}^{n\times n}$ is the gain matrix dependent on the error signal, and it is designed as

$$K_e = diag\{\frac{K_i}{\mathscr{D}_i^2 - e_i^2}\} \tag{12}$$

where K_i, $i \in \{1,\cdots,n\}$ denote positive gains. $K_r \in \mathbb{R}^{n\times n}$ denotes a constant, diagonal, positive definite control gain matrix, $\hat{\omega}(t) \in \mathbb{R}^{5n\times n}$ represents the estimated regressor matrix, and $\hat{\sigma}(\hat{\zeta},x) \in \mathbb{R}^{5n}$ denotes the estimated activation function. Here, $\hat{\zeta}(t) \in \mathbb{R}^{5n}$ refers to the estimated center of the activation function.

ARTICLE IN PRESS

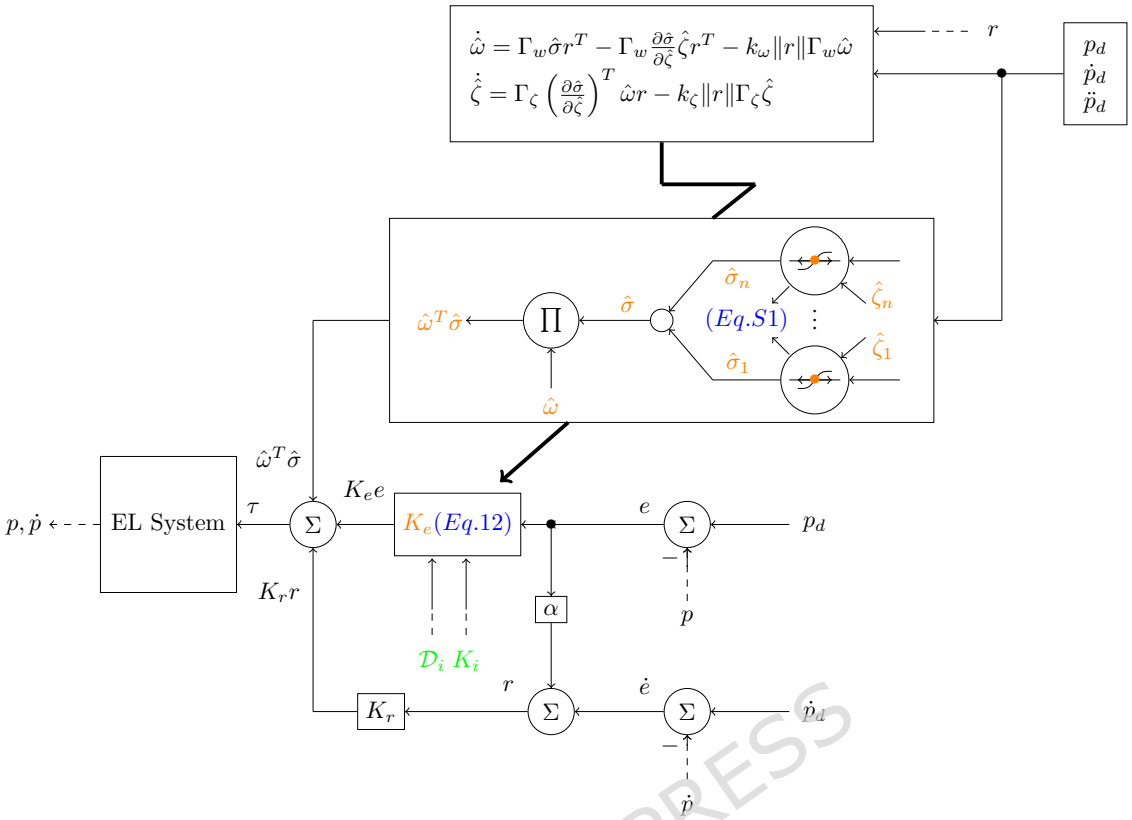

Figure 1. The block diagram of the closed loop system with the proposed adaptive NN structure. (see Supplementary Material Eq.S1)

Remark 1 *To improve the approximation of system uncertainties, we propose a specially designed, piecewise-defined activation function based on third-order polynomials. This function features an* adaptively shifting center *parameter, denoted by* ζ*, which allows the activation to dynamically align with varying operating conditions. The resulting function,* $\sigma(\zeta, x)$*, smoothly transitions between saturated regions at* -1 *and* $+1$*, and maintains continuity and differentiability over its entire domain. The explicit form and mathematical details of the proposed activation function are provided in Supplementary Material.*

The regressor matrix and center values are updated adaptively according to

$$\dot{\hat{\omega}} = \Gamma_\omega \hat{\sigma} r^T - \Gamma_\omega \frac{\partial \hat{\sigma}}{\partial \hat{\zeta}} \hat{\zeta} r^T - k_\omega \|r\| \Gamma_\omega \hat{\omega} \tag{13}$$

$$\dot{\hat{\zeta}} = \Gamma_\zeta \left(\frac{\partial \hat{\sigma}}{\partial \hat{\zeta}} \right)^T \hat{\omega} r - k_\zeta \|r\| \Gamma_\zeta \hat{\zeta} \tag{14}$$

where $\Gamma_\omega, \Gamma_\zeta \in \mathbb{R}^{5n \times 5n}$ are constant, positive definite, diagonal adaptation gain matrices, and $k_\omega, k_\zeta \in \mathbb{R}$ are constant, positive adaptation gains.

By substituting the control input design (11) into (10), we have closed-loop error dynamics as

$$M\dot{r} = \omega^T \sigma - \hat{\omega}^T \hat{\sigma} + \varepsilon + \tau_d - K_e e - K_r r - C_m r. \tag{15}$$

The schematic representation of the closed loop system is shown in Figure 1.

The self-adjusting update law in (14) can be interpreted as an online relocation of the activation centers toward the regions where the approximation error is dominant. This prevents the network from relying on static basis functions (as in conventional tanh based NNs) and instead enables a data-driven redistribution of the activation support during transients. Rather than using preselected basis sets, the proposed mechanism adaptively shifts the activation centers in real time, which enhances the approximation accuracy under time-varying uncertainties.

ARTICLE IN PRESS

4 Stability Analysis

In this section, based on the previously derived error dynamics, the stability of the closed-loop system will be investigated by employing Lyapunov-based analysis methods.

Theorem 1 *The proposed controller in (11), together with the parameter update laws in (13)–(14), ensures that all signals within the closed-loop system remains bounded and that the tracking error converges. This result holds provided the initial tracking error lies within a specified region.*

Proof 1 *To prove the Theorem 1, a nonnegative BLF* $\mathscr{V}(e,r,\tilde{\omega},\tilde{\zeta}) \in \mathbb{R}$ *is defined as*

$$\mathscr{V} \triangleq \frac{1}{2} r^T M r + \sum_{i=1}^{n} \frac{K_i}{2} ln\left(\frac{\mathscr{D}_i^2}{\mathscr{D}_i^2 - e_i^2}\right) + \frac{1}{2} tr\{\tilde{\omega}^T \Gamma_\omega^{-1} \tilde{\omega}\} + \frac{1}{2} \tilde{\zeta}^T \Gamma_\zeta^{-1} \tilde{\zeta} \tag{16}$$

where $\tilde{\omega}(t) \triangleq \omega - \hat{\omega} \in \mathbb{R}^{5n \times n}$ *and* $\tilde{\zeta}(t) \triangleq \zeta - \hat{\zeta} \in \mathbb{R}^{5n}$ *denote estimation errors and* $tr(\cdot)$ *shows trace of a matrix. By employing Property 1, one can derive that the following bound holds for (16)*

$$\frac{1}{2}\alpha_1 \|z\|^2 \leq \mathscr{V} \leq \frac{1}{2}\alpha_2 \|z\|^2 + c_{\mathscr{V}} \tag{17}$$

in which α_1, α_2, $c_{\mathscr{V}} \in \mathbb{R}$ *denote positive constants and are defined as* $\alpha_1 \triangleq min\{m_1, min\{K_i\}\}$, $\alpha_2 \triangleq max\{m_2, max\{K_i\}\}$ *and* $c_{\mathscr{V}} \triangleq \frac{1}{2}\lambda_{\max}\left(\Gamma_\omega^{-1}\right)\bar{\tilde{\omega}}^2 + \frac{1}{2}\lambda_{\max}\left(\Gamma_\zeta^{-1}\right)\bar{\tilde{\zeta}}^2$ *where* $\bar{\tilde{\omega}}$, $\bar{\tilde{\zeta}} \in \mathbb{R}$ *represent positive constants and ensured following inequalities* $\bar{\tilde{\omega}} \geq \|\tilde{\omega}\|_{i\infty}$, $\bar{\tilde{\zeta}} \geq \|\tilde{\zeta}\|$. *By utilizing (15) and Property 2, the time derivative of (16) can be obtained as follows*

$$\dot{\mathscr{V}} = r^T M \dot{r} + \frac{1}{2} r^T \dot{M} r + e^T K_e \dot{e} + tr\{\tilde{\omega}^T \Gamma_\omega^{-1} \dot{\tilde{\omega}}\} + \tilde{\zeta}^T \Gamma_\zeta^{-1} \dot{\tilde{\zeta}} \tag{18}$$

where $\sum_{i=0}^{n} K_i \frac{e_i \dot{e}_i}{\mathscr{D}_i^2 - e_i^2} = e K_e \dot{e}$ *was used. By utilizing the identity* $\omega^T \Phi - \hat{\omega}^T \hat{\Phi} = \tilde{\omega}^T \hat{\Phi} + \omega^T \tilde{\Phi}$, *and by canceling the common terms, we arrive at*

$$\dot{\mathscr{V}} = -e^T K_e \alpha e - r^T K_r r + r^T \tau_d + r^T \tilde{\omega}^T \hat{\Phi} + r^T \omega^T \tilde{\Phi} + r^T \varepsilon + tr\{\tilde{\omega}^T \Gamma_\omega^{-1} \dot{\hat{\omega}}\} + \tilde{\zeta}^T \Gamma_\zeta^{-1} \dot{\tilde{\zeta}}. \tag{19}$$

By employing the Taylor series expansion[29], following expression can be derived

$$\tilde{\Phi} = \frac{\partial \hat{\Phi}}{\partial \hat{\zeta}} \tilde{\zeta} + h \tag{20}$$

where $h(\zeta)$ *denotes high order terms. Substituting (20) and update rules (13) and (14) into (19) and by canceling the common terms yields*

$$\dot{\mathscr{V}} = -e^T K_e \alpha e - r^T K_r r + r^T \varepsilon + r^T \omega^T h + r^T \tau_d + tr\{k_\omega \|r\| \tilde{\omega}^T \hat{\omega}\} + r^T \tilde{\omega}^T \frac{\partial \hat{\Phi}}{\partial \hat{\zeta}} \zeta + \tilde{\zeta}^T k_\zeta \|r\| \hat{\zeta}. \tag{21}$$

The following bounds can be obtained[30]

$$r^T \omega^T h \leq \|r\| \|\omega\|_{i\infty} \|h\| \leq (a_0 + a_1 \|\tilde{\zeta}\|) \|r\| \tag{22}$$

$$r^T \tilde{\omega}^T \frac{\partial \hat{\Phi}}{\partial \hat{\zeta}} \zeta \leq a_2 \|\omega\|_{i\infty} \|r\| \tag{23}$$

where a_0, a_1, $a_2 \in \mathbb{R}$ *denote known positive constants. By employing the upper bounds (22) and (23), the right-hand side of (21) can be upper bounded as*

$$\begin{aligned} \dot{\mathscr{V}} \leq & -e^T K_e \alpha e - r^T K_r r + r^T \varepsilon + (a_0 + a_1 \|\tilde{\zeta}\|) \|r\| + a_2 \|\omega\|_{i\infty} \|r\| + [k_\omega tr\{\tilde{\omega}^T \omega\} - k_\omega tr\{\tilde{\omega}^T \tilde{\omega}\}] \|r\| \\ & + [k_\zeta \tilde{\zeta}^T \zeta - k_\zeta \tilde{\zeta}^T \tilde{\zeta}] \|r\| + r^T \tau_d. \end{aligned} \tag{24}$$

By applying the bounds $\|\omega\|_{i\infty} \leq \bar{\omega}$, $\|\zeta\| \leq \bar{\zeta}$, *where* $\bar{w}, \bar{\zeta}$ *are positive constants, and subsequently completing the squares, one obtains*

$$\dot{\mathscr{V}} \leq -e^T K_e \alpha e - r^T K_r r + \|r\| \left[a_0 + \varepsilon + \tau_d + \frac{(a_2 + k_\omega \bar{\omega})^2}{4 k_\omega} + \frac{(a_1 + k_\zeta \bar{\zeta})^2}{4 k_\zeta} \right]. \tag{25}$$

ARTICLE IN PRESS

The right hand side of (25) can further be upper bounded as

$$\dot{\mathscr{V}} \leq -\beta\|z\|^2 + \frac{\gamma^2}{4\kappa} \tag{26}$$

for positive constants $\beta \triangleq min\{\lambda_{min}(K_e\alpha), \lambda_{min}(K_r) - \kappa)\}$ *where* $\lambda_{min}\{\cdot\}$ *denotes minimum eigenvalue of a matrix and* $\gamma\|r\| \leq \frac{\gamma^2}{4\kappa} + \kappa\|r\|^2$ *was made use of for a positive damping constant* κ*.*

From structure (17) and (26), it can be demonstrated that $\mathscr{V}(t) \in \mathscr{L}_\infty$*, thereby establishing that (5) and (6) are bounded. By employing standard signal-chasing arguments, it can be demonstrated that all signals remain bounded under closed-loop operation. Also, from (17) and (26), UUB of (5) and (6) is ensured with the ultimate bounds determined by the constants on the right-hand sides of (17) and (26). Furthermore, the boundedness result directly follows from* $\mathscr{V}(t) \in \mathscr{L}_\infty$*, which guarantees that all closed-loop signals remain finite for all* $t > 0$*. The subsequent inequality quantifies the ultimate bound explicitly. By substituting the upper bound of (17) into (26), one obtains* $\dot{\mathscr{V}} \leq -\frac{2\beta}{\alpha_2}\mathscr{V} + \frac{2\beta}{\alpha_2}c_{\mathscr{V}} + \frac{\gamma^2}{4\kappa}$*. Solving this differential inequality yields* $\mathscr{V}(t) \leq \mathscr{V}(0)e^{-\frac{2\beta}{\alpha_2}t} + \left(c_{\mathscr{V}} + \frac{\alpha_2}{8\kappa\beta}\gamma^2\right)\left(1 - e^{-\frac{2\beta}{\alpha_2}t}\right)$*. Hence, the tracking error satisfies the UUB condition in the sense that* $\|e(t)\| \leq \sqrt{\frac{2}{\alpha_1}\left(c_{\mathscr{V}} + \frac{\alpha_2}{8\kappa\beta}\gamma^2\right)}$*, as* $t \to \infty$*, where the constants* β*,* γ*, and* κ *depend on the control and adaptation gains. These constants can be adjusted through control and adaptation gains, ensuring practical tracking of the desired position vector.*

Remark 1. *BLF incorporated in the stability analysis provides a rigorous mechanism to enforce error constraints. Unlike conventional Lyapunov functions that merely establish boundedness, the BLF term approaches infinity as the tracking error tends to the predefined boundary. This singularity property prevents the error trajectory from crossing the admissible limits, thereby guaranteeing that the tracking error remains strictly within the constrained region for all* $t > 0$*, provided the initial condition lies inside it. Furthermore, the proposed adaptive NN with self-adjusting activation centers improves the compensation of time-varying uncertainties, which reduces the likelihood of the error approaching the boundary and enhances robustness of the closed-loop system.*

5 Simulation Results

To evaluate the performance of the proposed NN based robust control scheme, a set of comparative simulations was conducted on a two degree of freedom planar robotic manipulator. The simulations utilized the dynamic formulation described in (1), with system parameters adapted from established references such as[31]

$$M = \begin{bmatrix} \theta_1 + 2\theta_2 c_2 & \theta_2 + \theta_3 c_2 \\ \theta_2 + \theta_3 c_2 & \theta_2 \end{bmatrix} \tag{27}$$

$$C_m = \begin{bmatrix} -\theta_3 s_2 \dot{q}_2 & -\theta_3 s_2(\dot{q}_1 + \dot{q}_2) \\ \theta_3 s_2 \dot{q}_1 & 0 \end{bmatrix} \tag{28}$$

$$G = \begin{bmatrix} \theta_4 c_1 + \theta_5 c_{12} \\ \theta_3 s_2 \dot{q}_1 \end{bmatrix} \tag{29}$$

$$F_d = \begin{bmatrix} \theta_6 & 0 \\ 0 & \theta_7 \end{bmatrix} \tag{30}$$

$$\tau_d = \begin{bmatrix} sin(0.2t) \\ cos(0.2t) \end{bmatrix} \tag{31}$$

where $\theta_1 = 3.473$, $\theta_2 = 0.193$, $\theta_3 = 0.242$, $\theta_4 = 12.936$, $\theta_5 = 3.528$, $\theta_6 = 5.3$, $\theta_7 = 1.1$ and $s_2 = \sin(q_2)$, $c_2 = \cos(q_2)$, $c_{12} = \cos(q_1 + q_2)$. In the course of numerical simulations, consistent with prior analyses, model parameters are treated as uncertain and thus excluded from the control synthesis process. Accordingly, the target joint position vector is defined as

$$q_d = \begin{bmatrix} 0.3\sin(1.5t)(1 - \exp(-0.1t^2)) \\ 0.3\sin(1.5t)(1 - \exp(-0.1t^2)) \end{bmatrix} [\text{rad}]. \tag{32}$$

The controller gains were adjusted as $K_r = 60I_2$, $\alpha = 5I_2$, $K_i = 1.1I_2$ and the adaptation gains were assigned as $\Gamma_\omega = 100$, $\Gamma_\zeta = 200$, $k_\omega = 0.001$, and $k_\zeta = 1.1$.

ARTICLE IN PRESS

To approximate the system uncertainties, a NN architecture with a single hidden layer was employed. Instead of standard activation functions, the proposed piecewise third-order polynomial-based activation function with an adaptively shifting center ζ was utilized, as detailed in Supplementary Material.

The robot manipulator is initially configured in a stationary state, with both joint angles set to 0.5°. In all simulation studies, the initial tracking errors were chosen inside the admissible region, in accordance with the BLF-based formulation. To examine the impact of position constraints on tracking performance, the constraint bounds $\mathscr{D}_i$, where $i \in \{1,2\}$, are adjusted to values of 1°, 2°, and 3° in separate simulation cases. It is noted that while all computations are performed in radians, the results are presented in degrees for clarity.

The simulation results for $\mathscr{D}_i \equiv 1^\circ$ are presented in Figures 2 and 3, where Figure 2 illustrates the joint position tracking errors and Figure 3 shows the corresponding control input torques.

For the case $\mathscr{D}_i \equiv 2^\circ$, Figures 4 and 5 provide the tracking error and control input results, respectively. Similarly, the outcomes for $\mathscr{D}_i \equiv 3^\circ$ are depicted in Figures 6 and 7.

As seen in Figures 2, 4, and 6, the proposed controller ensures accurate trajectory tracking while satisfying the imposed position constraints. Even as the constraints become less restrictive (i.e., larger $\mathscr{D}_i$ values), the controller maintains stable and bounded behavior, demonstrating its adaptability and robustness in handling varying joint position limits.

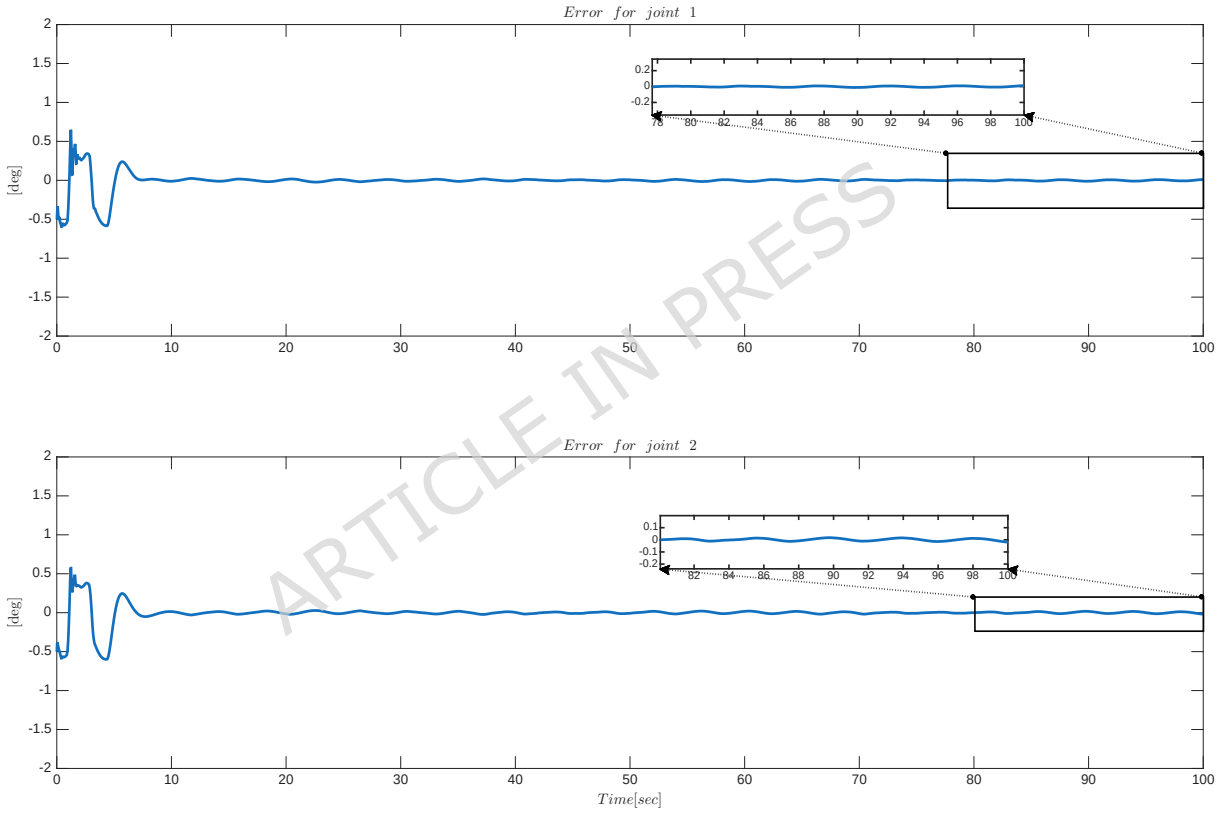

Figure 2. Joint position tracking error $e(t)$. ($\mathscr{D}_i \equiv 1^\circ$)

Another comparative study was performed using the proposed controller structure with two different activation functions given in Figure 8: the newly introduced self-adjusted activation function and the classical tanh function. This additional analysis aims to evaluate the influence of the activation function design on the overall control performance and tracking accuracy. The results of this comparative study are presented in Table 1. As can be observed, employing the proposed self-adjusted activation function leads to lower total tracking error and reduced overall control effort compared to the conventional tanh activation function.

For a fair comparison with an optimal controller, a baseline LQR was designed on the nominal decoupled error dynamics $\dot{x} = Ax + Bu$, where $A = \begin{bmatrix} 0 & I \\ 0 & 0 \end{bmatrix}$ and $B = \begin{bmatrix} 0 \\ I \end{bmatrix}$, with the state vector defined as $x = [e^\top, \dot{e}^\top]^\top$. This simplified double-integrator model was used instead of the full nonlinear robot dynamics to provide a standard optimal control benchmark. Using $Q = \mathrm{diag}(q_e I, q_{\dot{e}} I)$ and $R = rI$, the optimal feedback gain $K = [K_p \; K_d]$ was obtained by solving the continuous-time Riccati

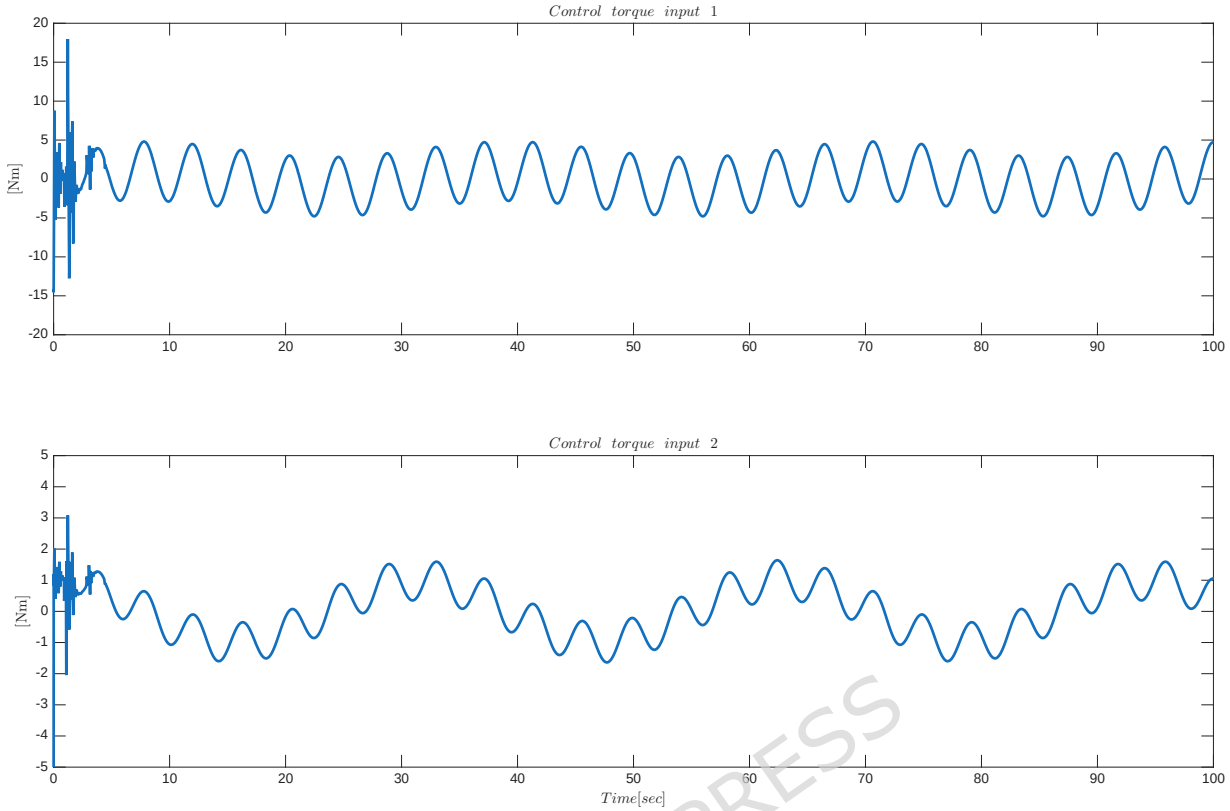

Figure 3. Control input torque $\tau(t)$. ($\mathscr{D}_i \equiv 1^\circ$)

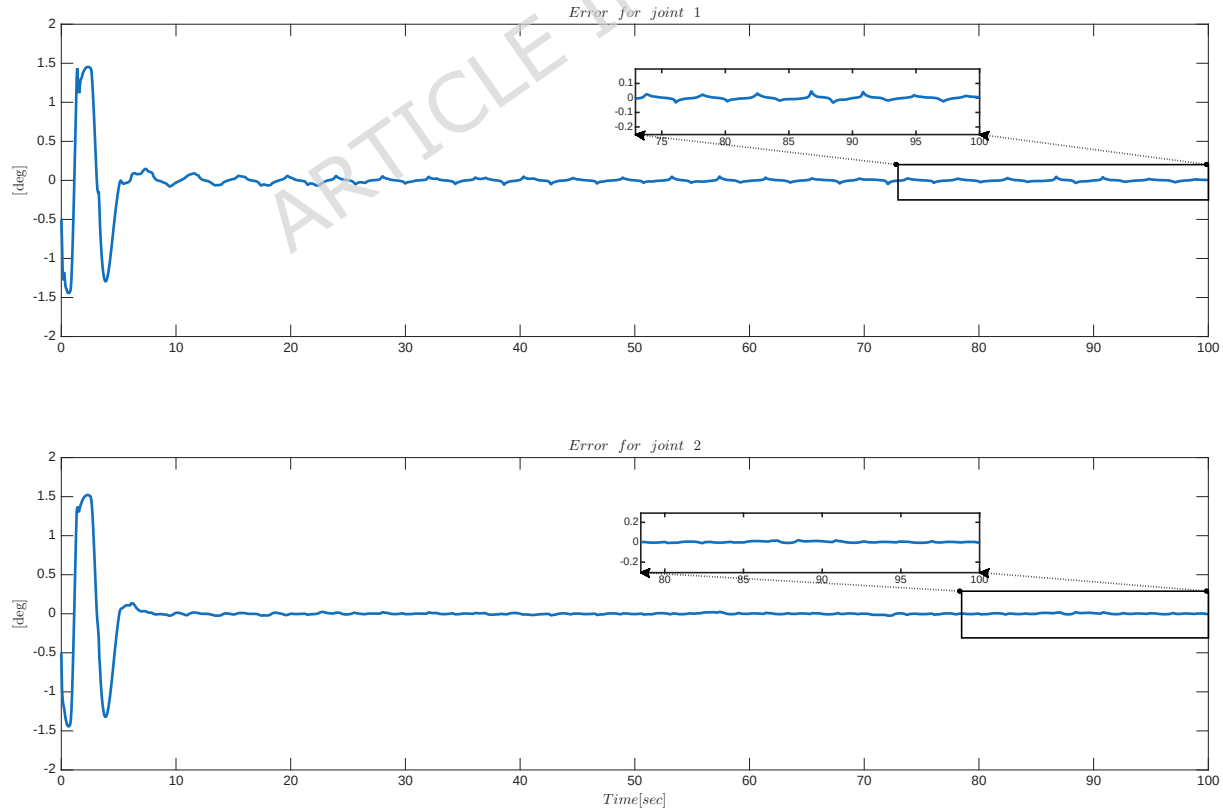

Figure 4. Joint position tracking error $e(t)$. ($\mathscr{D}_i \equiv 2^\circ$)

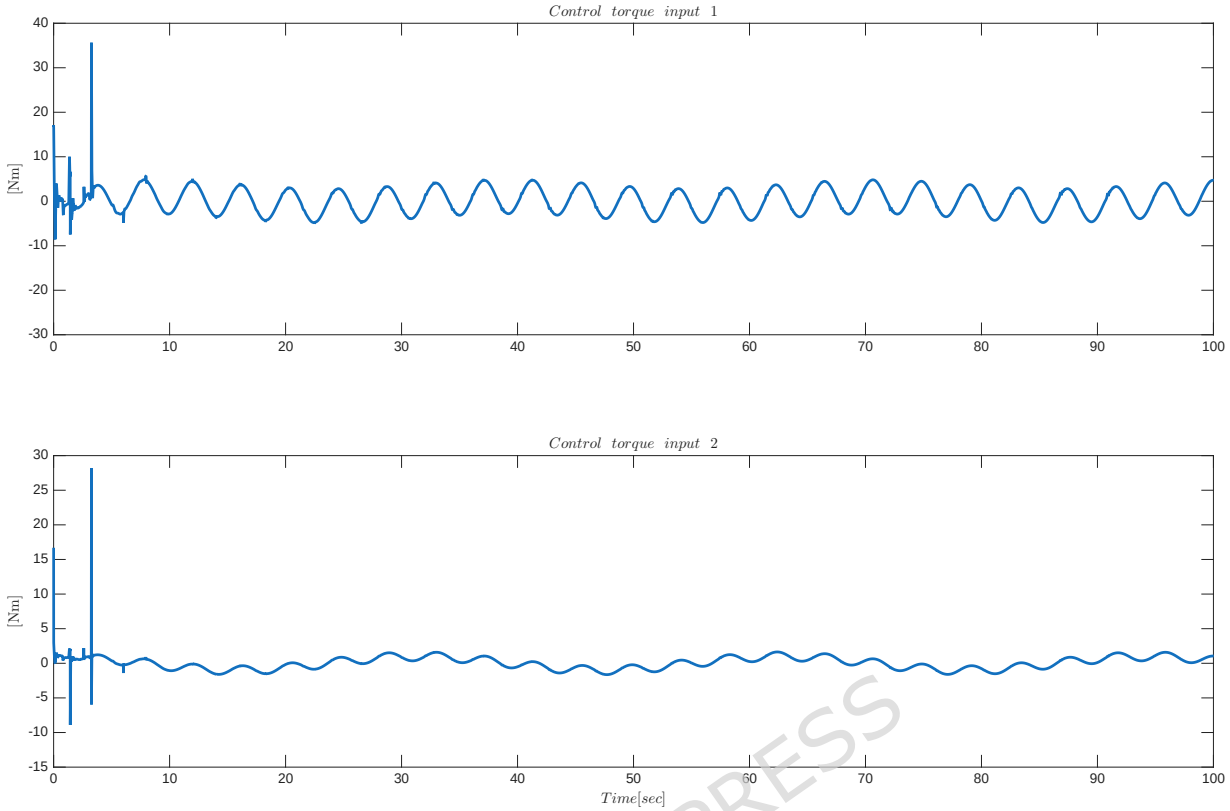

Figure 5. Control input torque $\tau(t)$. ($\mathscr{D}_i \equiv 2^\circ$)

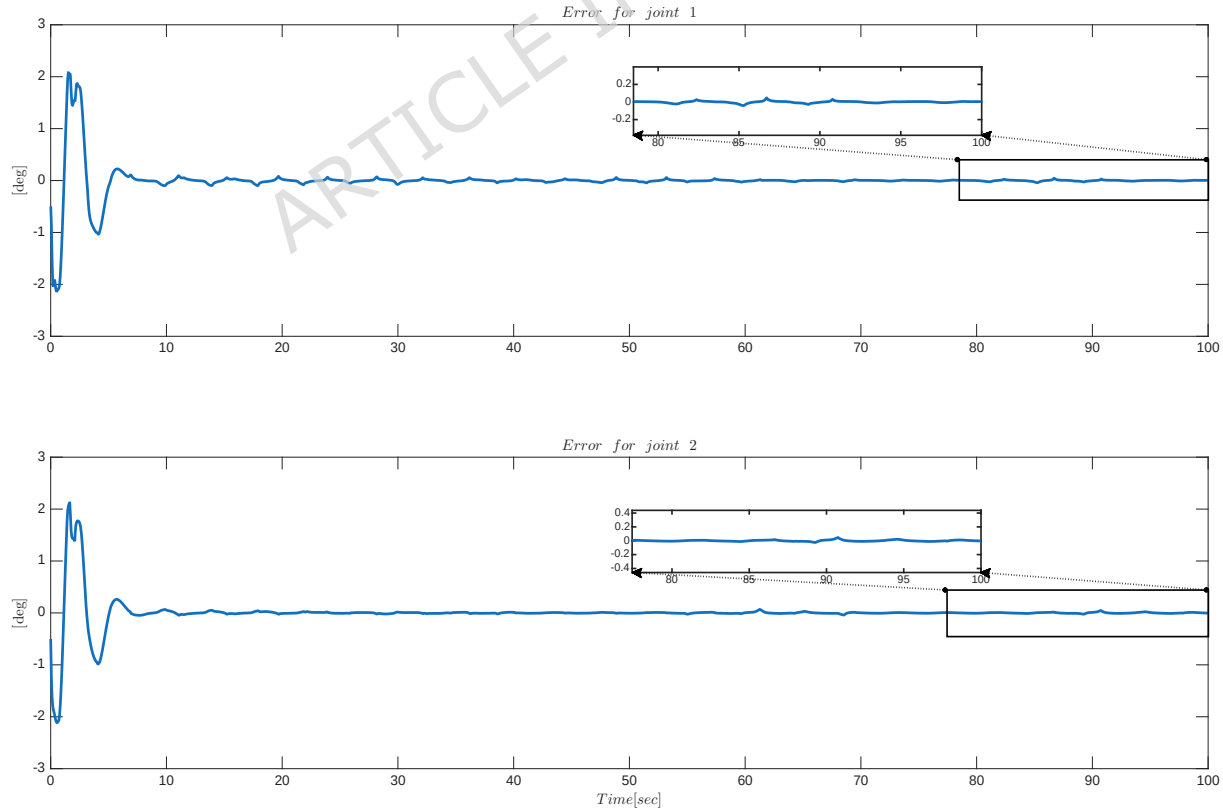

Figure 6. Joint position tracking error $e(t)$. ($\mathscr{D}_i \equiv 3^\circ$)

ARTICLE IN PRESS

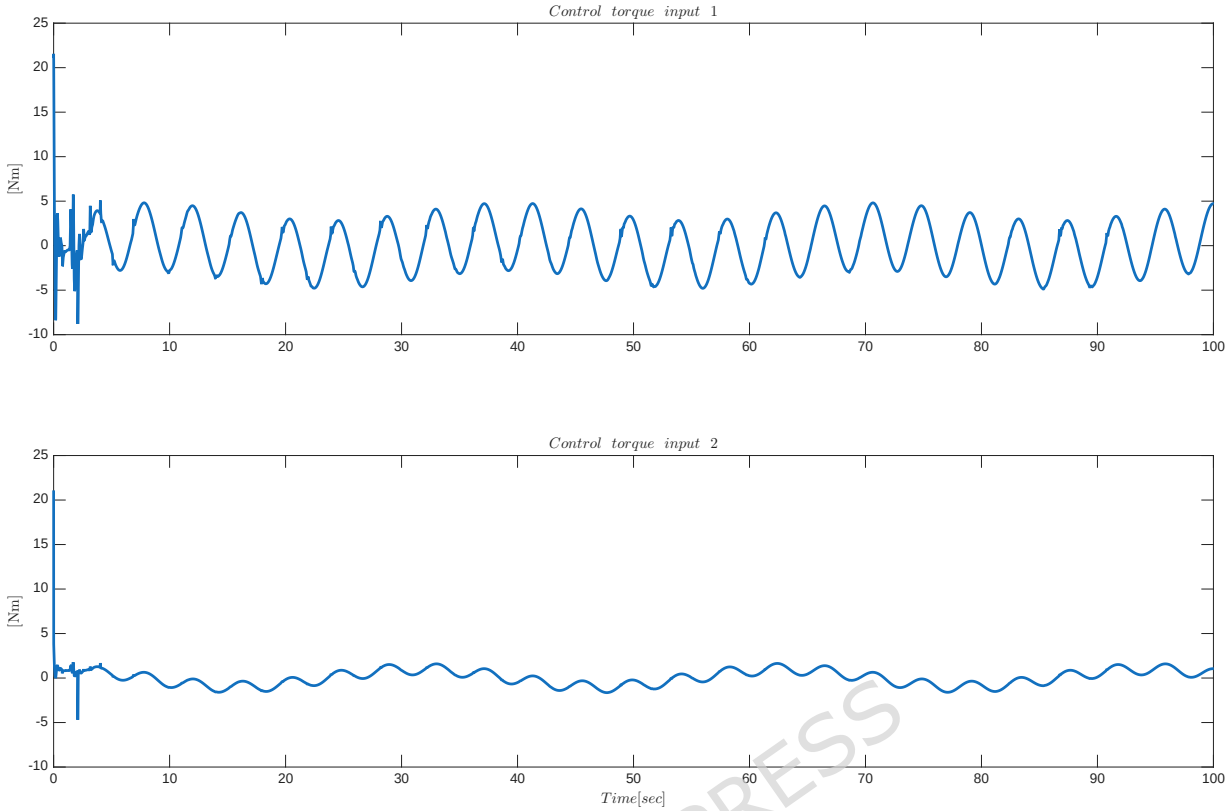

Figure 7. Control input torque $\tau(t)$. ($\mathscr{D}_i \equiv 3^\circ$)

equation. For the chosen parameters, this yielded $K_p = \begin{bmatrix} 948.68 & 0 \\ 0 & 948.68 \end{bmatrix}$ and $K_d = \begin{bmatrix} 129.99 & 0 \\ 0 & 129.99 \end{bmatrix}$, leading to the control law $u_{\text{LQR}} = -K_p e - K_d \dot{e}$. Both the proposed controller and the LQR baseline were tested under identical reference trajectories and disturbances. As shown in Figure 8 and Table 1, the proposed controller consistently achieved lower tracking error while requiring less control effort, highlighting the advantages of the BLF-based constraint enforcement and the adaptive NN structure, which provide robustness to uncertainties and precise error regulation within predefined bounds.

Table 1. Comparative Analysis of Performance Metrics for the First Example

Type of controller	$\int \|\|e(v)\|\|^2 dv$	$\int \|\|u(v)\|\|^2 dv$
Proposed controller with new activation function	2.636	3484
Proposed controller with tanh function	3.265	3749
LQR controller	3.447	4075

6 Conclusion

In this study, a novel robust control strategy with position constraints has been developed for Euler–Lagrange systems subject to dynamic uncertainties and external disturbances. The proposed controller combines a nonlinear robust control law with an adaptive NN-based estimator that incorporates automatically adjusting activation functions. These activation functions are designed with iteratively updated centers, enhancing the network's ability to approximate time-varying and nonlinear uncertainties without requiring linear parameterization or predefined activation sets. Unlike traditional adaptive NNs that rely on fixed Gaussian basis functions, the proposed method directly adjusts activation centers online at each iteration, thereby improving estimation accuracy near non-smooth regions. To enforce state constraints on joint positions, a BLF-based approach is employed, ensuring that the tracking error remains within a predefined region, provided it starts within it. The stability of

ARTICLE IN PRESS

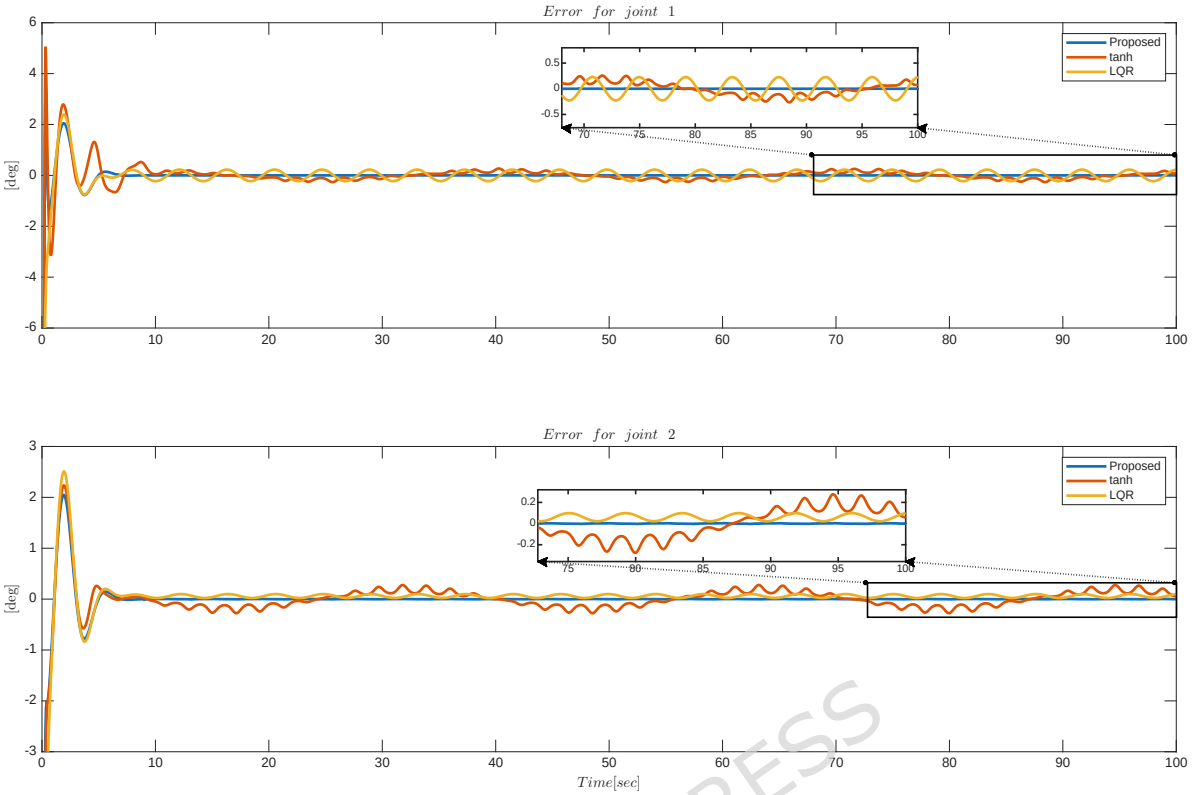

Figure 8. Comparison of joint position tracking error $e(t)$ obtained using the proposed self-adjusted activation function and the conventional tanh activation function.

the overall system is rigorously analyzed using a Lyapunov-based framework, establishing uniform ultimate boundedness of all closed-loop signals. Comparative numerical simulations validate the effectiveness and robustness of the proposed control architecture under significant uncertainty and disturbance scenarios. Future research will focus on real-time experimental validation and on extending the proposed approach to more complex Euler–Lagrange systems, including manipulators with additional degrees of freedom and systems subject to strong nonlinear friction. Another promising direction is the rigorous integration of input constraints into the stability analysis. In particular, incorporating explicit bounds on the control torque would not only prevent potential singularities in the input channel but also provide stronger theoretical guarantees on precision and safety.

Data availability

The data is available from the corresponding author on reasonable request.

Methods

The MATLAB code used to generate the simulation results in this study is available from the corresponding author upon reasonable request.

References

1. He, D., Wang, H., Tian, Y. & Fliess, M. Mimo ultra-local model-based adaptive enhanced model-free control using extremum-seeking for coupled mechatronic systems. *ISA transactions* (2024).
2. Chen, J., Lyu, L., Fei, Z., Xia, W. & Sun, X.-M. Event-triggered adaptive robust control for a class of uncertain nonlinear systems with application to mechatronic system. *IEEE Transactions on Ind. Informatics* **19**, 11800–11808 (2023).
3. Patre, P. M., MacKunis, W., Dupree, K. & Dixon, W. E. Modular adaptive control of uncertain euler–lagrange systems with additive disturbances. *IEEE Transactions on Autom. Control.* **56**, 155–160 (2010).

ARTICLE IN PRESS

4. Liu, H., Tian, Y., Lewis, F. L., Wan, Y. & Valavanis, K. P. Robust formation tracking control for multiple quadrotors under aggressive maneuvers. *Automatica* **105**, 179–185 (2019).
5. Huang, G. *et al.* Robust optimal tracking control of multiple autonomous underwater vehicles subject to uncertain disturbances. *IET Control. Theory & Appl.* (2024).
6. Inci, H., Selim, E., Tatlicioglu, E., Zergeroglu, E. & Savran, A. A saturation based self-tuned robust control design for euler lagrange systems. *ISA transactions* (2024).
7. Patre, P. M., MacKunis, W., Johnson, M. & Dixon, W. E. Composite adaptive control for euler–lagrange systems with additive disturbances. *Automatica* **46**, 140–147 (2010).
8. Ünver, Ş., Selim, E., Tatlıcıoğlu, E., Zergeroğlu, E. & Alcı, M. Adaptive control of bldc driven robot manipulators in task space. *IET Control. Theory & Appl.* (2024).
9. Zhang, H., Zhao, Y., Wang, Y. & Liu, L. Adaptive neural network control of robotic manipulators with input constraints and without velocity measurements. *IET Control. Theory & Appl.* (2024).
10. Jiang, B. *et al.* Neural network based model predictive control for a quadrotor uav. *Aerospace* **9**, 460 (2022).
11. Fang, Y., Zhang, J. & Li, Y. Neural networks adaptive predefined-time control for pure-feedback nonlinear systems: a case study on robotic exoskeleton systems. *Sci. Reports* **15**, 6041 (2025).
12. Adiche, S. *et al.* Advanced control strategy for ac microgrids: a hybrid ann-based adaptive pi controller with droop control and virtual impedance technique. *Sci. Reports* **14**, 31057 (2024).
13. Wang, H., Chen, B., Lin, C., Sun, Y. & Wang, F. Adaptive finite-time control for a class of uncertain high-order non-linear systems based on fuzzy approximation. *IET Control. Theory & Appl.* **11**, 677–684 (2017).
14. Wu, Y., Yang, X., Yan, H., Chadli, M. & Wang, Y. Adaptive fuzzy event-triggered sliding-mode control for uncertain euler–lagrange systems with performance specifications. *IEEE Transactions on Fuzzy Syst.* **31**, 1566–1579 (2022).
15. Wang, C., Liang, J. & Deng, Q. Dynamics of heterogeneous hopfield neural network with adaptive activation function based on memristor. *Neural Networks* **178**, 106408 (2024).
16. Jagtap, A. D., Kawaguchi, K. & Karniadakis, G. E. Adaptive activation functions accelerate convergence in deep and physics-informed neural networks. *J. Comput. Phys.* **404**, 109136 (2020).
17. Jagtap, A. D., Shin, Y., Kawaguchi, K. & Karniadakis, G. E. Deep kronecker neural networks: A general framework for neural networks with adaptive activation functions. *Neurocomputing* **468**, 165–180 (2022).
18. Tee, K. P., Ge, S. S. & Tay, E. H. Barrier lyapunov functions for the control of output-constrained nonlinear systems. *Automatica* **45**, 918–927 (2009).
19. Li, Y.-X. Barrier lyapunov function-based adaptive asymptotic tracking of nonlinear systems with unknown virtual control coefficients. *Automatica* **121**, 109181 (2020).
20. Cruz-Ortiz, D., Chairez, I. & Poznyak, A. Sliding-mode control of full-state constraint nonlinear systems: A barrier lyapunov function approach. *IEEE Transactions on Syst. Man, Cybern. Syst.* **52**, 6593–6606 (2022).
21. Sun, W., Su, S.-F., Wu, Y., Xia, J. & Nguyen, V.-T. Adaptive fuzzy control with high-order barrier lyapunov functions for high-order uncertain nonlinear systems with full-state constraints. *IEEE Transactions on Cybern.* **50**, 3424–3432 (2019).
22. Gul, S., Zergeroglu, E. & Tatlicioglu, E. Robust task space position constraint control of kinematically redundant manipulators: A barrier lyapunov approach. *Transactions Inst. Meas. Control.* 01423312241296968 (2024).
23. Pan, C., Huang, H., Chen, C., Wu, L. & Xiao, J. Neuro-adaptive command-filtered backstepping control of uncertain flexible-joint manipulators with input saturation via output. *Sci. Reports* **15**, 1–21 (2025).
24. Bey, O., Amirat, Y. & Mohammed, S. Adaptive model-free control for ankle-assistive orthosis: A robust approach to real-time gait tracking. *Mechatronics* **109**, 103341 (2025).
25. Bey, O. & Chemachema, M. Finite-time event-triggered output-feedback adaptive decentralized echo-state network fault-tolerant control for interconnected pure-feedback nonlinear systems with input saturation and external disturbances: A fuzzy control-error approach. *Inf. Sci.* **669**, 120557 (2024).
26. Ortega, R. *et al. Euler-Lagrange systems* (Springer, 1998).
27. Castro, J. L. Fuzzy logic controllers are universal approximators. *IEEE Tr. on Syst. Man, Cybern.* **25**, 629–635 (1995).
28. Wang, L.-X. Fuzzy systems are universal approximators. In *IEEE Int. Conf. on Fuzzy Systems*, 1163–1170 (1992).

ARTICLE IN PRESS

ARTICLE IN PRESS

29. Kreyszig, E. *Advanced Engineering Mathematics* (Wiley, 2009).

30. Commuri, S. & Lewis, F. L. Adaptive-fuzzy logic control of robot manipulators. In *IEEE Int. Conf. on Robotics and Automation*, 2604–2609 (Minneapolis, MN, USA, 1996).

31. Lewis, F. L., Dawson, D. M. & Abdallah, C. T. *Robot Manipulator Control: Theory and Practice* (CRC Press, 2003).

Author contributions statement

B.M.Y: Conceptualization, Investigation, Software, Writing, Review and editing.

Funding

This research received no external funding.

Declarations

Competing interests

The authors declare no competing interests.

ARTICLE IN PRESS